

Multi-Active Bridge Based DC-Link Balancing of Three-Level NPC Inverters

Ferdinand Grimm^{1*}, Pouya Kolahian¹, Richard Bucknall¹ and Mehdi Baghdadi¹

¹Department for Mechanical Engineering, University College London, London, UK

*E-mail: ferdinand.grimm.18@ucl.ac.uk

Keywords: NEUTRAL POINT CLAMPED INVERTER, DC-LINK BALANCING, MULTI-ACTIVE BRIDGE

Abstract

A common topic in multilevel converter research is the question of DC-link capacitor voltage balancing. For the three-level neutral point clamped converter the balancing is difficult due to the nonlinear nature of the DC-link capacitor voltages. Previous papers solved this problem using sophisticated controllers or additional circuitry connected in parallel to the load. Those solutions however restrict the performance of the output voltage since the controller has to provide a trade-off between output voltage performance and DC-link balancing while the load-connected balancing circuit puts limitations on the applied modulation scheme. In this paper, we connect a multi-active bridge circuit to the DC-link of the converter to overcome this problem. The proposed method is independent of the modulation scheme of the neutral point clamped converter and allows to use of all possible switching states to control the output voltage without taking the effect on the DC-link balance into account. The efficiency of the proposed method is verified using experimental results.

1 Introduction

A promising multilevel inverter topology is the Three-level neutral point clamped (NPC) inverter which has first been introduced in [1]. Based on this topology, many variants of the Three-level topology as well as extensions for example for more variants have been proposed. A discussion of those variants and multilevel extensions (shown e.g. in Fig. 1) of the NPC converter is given in [2]. A special focus has been set to integrate the three-level NPC converter to electric drivetrains, and promising results can be found e.g. in [3]. Moreover, the NPC has been found as one of the most competitive three-level topologies for automotive drives as stated in [4].

The NPC converter gives several advantages over regular two-level B6 bridges such as a greater number of output levels and reduced voltage stress of the switches. However it comes with several disadvantages such as the need for the DC-link capacitor voltages to be balanced which would otherwise lead to bad dynamic performance and high voltage stress [5–10]. A mathematical derivation of the dynamics of the DC-link capacitor voltages can for example be found in [5]. Unbalanced DC-link capacitors yield distorted waveforms which in turn reduces the dynamic performance of the converter. For this reason, several solutions have been proposed in the literature. Carrier-based PWM is using different subcarrier signals to control the DC-link balance of the converter [6]. A phase-shift based control for the neutral point voltage of the NPC can be found in [7]. This control method provides good performance for smaller unbalance. The more DC-link unbalance, however, the worse the performance of the converter. For this reason, this method provides a great solution for applications with smaller unbalance. Space-Vector PWM is summarizing the number of applicable switching states into groups according to their effect

on the DC-link balance. While some of the vectors have no influence or are not predictable, certain switching states will always increase or decrease the neutral point voltage. Using this scheme, it is possible to restrict the pool of candidate switching states to only those which lead to a minimization of the DC-link voltage difference [8]. However, restricting the pool of candidates might also exclude the optimal solution for the output voltage. For this reason, space vector modulation will only provide a trade-off between DC-link balancing and output voltage tracking. In addition to the presented DC-link balancing schemes, a model predictive control strategy can be used as well where the future DC-link balance is predicted from its system model and then the switching state candidate that yields the best DC-link balance is chosen [9]. Since the output voltage has to be controlled as well, it is necessary to find a trade-off between the DC-link balance and the performance of the output voltage in this case. This is usually achieved by using a cost function that is given as a weighted sum of the two control goals [9]. While the aforementioned control strategies work well on Three-level NPC topologies, their complexity tremendously increases for multilevel inverters as can be seen from the adaption of those methods to higher level NPC inverter versions [10]. This motivates the usage of different approaches for NPC topologies with a large number of output levels.

As an alternative to the presented control algorithms, it is possible to use an external balancing circuit as shown in [11–13]. The authors of [11] suggested placing an RLC circuit in parallel with the load and thus achieving balancing using currents through the switches. However, the presented method is dependent on the modulation scheme and the performance is varying with the output voltage frequency. In [12] a special DC/DC boost topology has been used to balance the capacitors. This

topology is independent of the modulation and the load, however, the proposed topology needs a combined voltage and current controller that matches the switching state of the boost converter with the DC-link unbalance of the NPC converter. Furthermore, balancing more than one capacitor at the same time is difficult with the proposed topology. Instead of a boost-converter topology, it is possible to use a switched-capacitor converter for external balancing as demonstrated in [13]. However, the switched capacitor topology is only capable to balance one type of unbalance at a time.

Another balancing topology, the multi-active bridge shown in Fig. 2 has recently been given increased attention [14–18]. The multi-active bridge is a DC/DC topology consisting of several active bridges which are magnetically connected [14]. In case all windings are connected with the same magnetic flux and identical turns number, the AC-voltage of all modules is identical and thus the DC-voltage will be identical as well achieving perfect balancing. A system model for the internal dynamics of the multi-active bridge for this connection type can for example be found in [15]. The balancing potential of the multi-active bridge makes it ideal for multilevel converter applications which otherwise require a complicated controller that would furthermore restrict the switching states which are permitted to control the load voltage [16]. In this way, a successful battery balancing system based on the multi-active bridge has been proposed in [17]. A major difference compared to the balancing circuit presented in [11] is that the multi-active bridge can be connected to the DC-side and therefore is independent of the modulator or output frequency. In addition to that, the switching losses of the multi-active bridge can be greatly reduced by applying specialized gate drivers with zero voltage switching [18]. While the multi-active bridge based balancing has been proven to be effective for balancing the DC voltages of various circuits, it is not researched very well for conventional multilevel converter topologies such as the NPC converter.

For this reason, a multi-active bridge based balancing topology for the NPC converter is proposed in this work. The remainder of this paper is organized as follows: Section 2 presents the proposed topology. Experiment results are given in Section 3 and the modulation for the proposed converter topology can be found in Section 4. Section 5 gives the conclusions.

2 Proposed System Topology

The complete system considered in this paper is shown in Fig. 3. It consists of five parts, the voltage source, the multi-active bridge, the NPC and the RL - load. The setup is fed by a DC-source that provides a constant supply V_{DC} . Both terminals of the DC-source are connected to an NPC phase leg. The NPC phase leg is converting the voltage to AC and feeds it to a series RL - load consisting of R_L and L_L . While this setup would be sufficient to produce an AC voltage at the output, it would not ensure keeping the DC-link capacitors balanced without the use of a dedicated controller. Therefore, a multi-active bridge is attached as an external circuit to ensure the DC-link capacitor

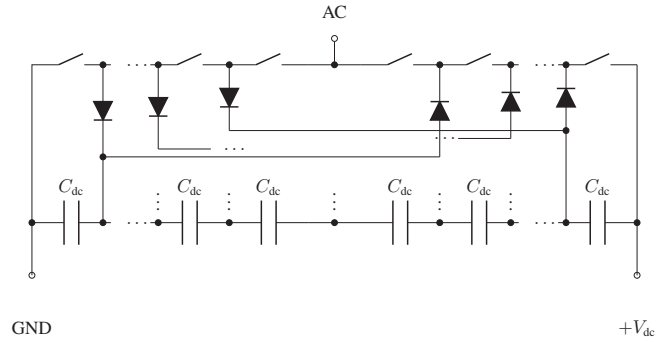


Fig. 1 Circuit Diagram of a multi-level diode clamped NPC converter with ideal switches.

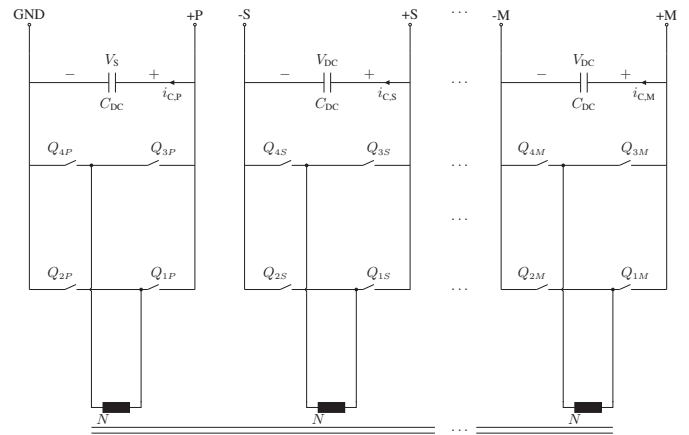


Fig. 2 Circuit Diagram of a Multi-Active Bridge with M modules and ideal switches.

voltage balancing. To keep the DC-link capacitors C_{DC_1} and C_{DC_2} of the NPC balanced, each of them is connected to the DC-terminals of an active bridge. The active bridges convert the DC voltage to AC. In the AC domain, both active bridges are connected magnetically through the windings of a multi-winding transformer. If all windings share the same core and have an equal amount of flux passing through them, the AC-voltage V_{mid} of all active bridges will be identical. An identical AC voltage on all active bridges will result in an identical DC voltage of the active bridges. Since each bridge is connected in parallel to a DC-link capacitor, this will achieve balanced DC-link capacitor voltages.

While Fig. 3 shows the case for a Three-level NPC inverter, the proposed topology can be extended to multilevel NPC inverters such as the one shown in Fig. 1 by using additional multi-active bridges and connecting each of them to one of the DC-link capacitors of the NPC converters. In this way, it is possible to balance arbitrarily large inverter topologies without the use of a balancing controller or decrease in performance. As the computational complexity of DC-link controllers greatly increases with the number of modules present in the converter, the proposed setup is especially useful for very large scale multilevel inverters consisting of many modules.

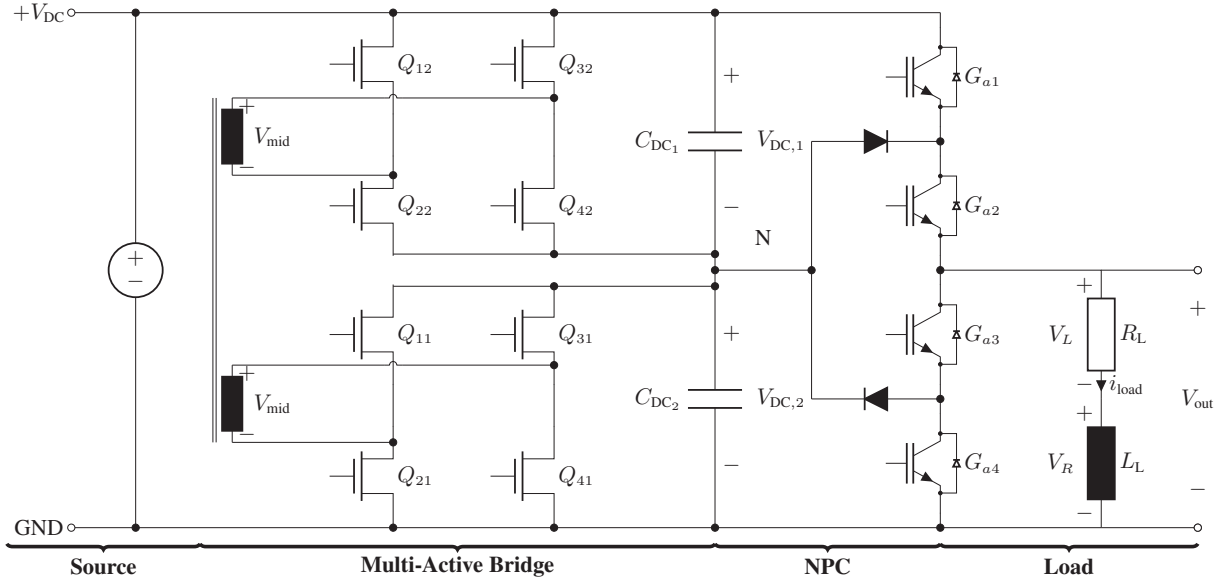


Fig. 3 Circuit Diagram of the proposed setup consisting of a Multi-Active Bridge connected to an NPC converter for DC-link balancing. The system is divided into four parts: The DC-source, the Multi-Active Bridge, the NPC phase leg and the RL - Load. GND refers to the reference voltage and N to the neutral point of the NPC converter.

3 Modulation and Control Techniques

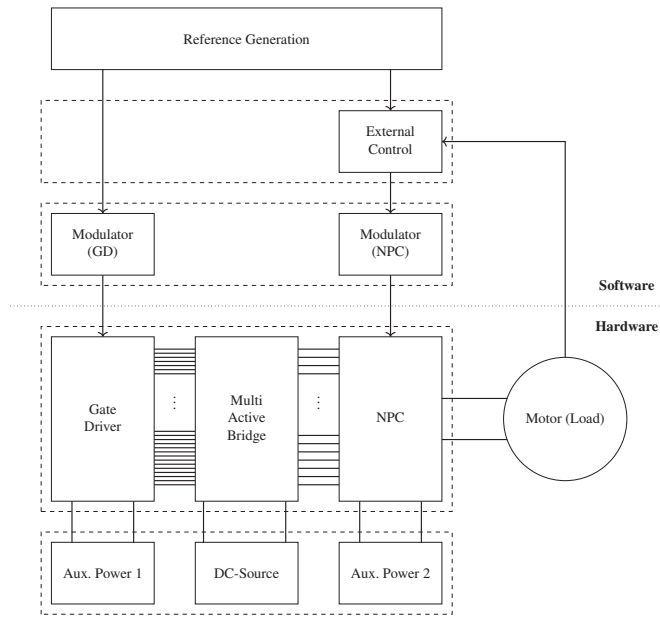


Fig. 4 Overview over the proposed balancing topology with its control scheme. From top to bottom the component categories are shown in dashed boxes. Starting with the controller, followed by the modulator, the physical system and the power supply. Furthermore, the converter is composed of three major parts: From left to right are shown the gate driver, the multiactive bridge and the NPC. The connections show how the component categories interact with each other for the different subsystems.

An overview over the control of the system is shown in Fig. 4. The proposed topology consists of a considerably larger number of switches compared to a conventional diode-clamped NPC converter. It is therefore necessary to take an additional modulation scheme for the multi-active bridge into account. Contrary to existing DC-link controllers, the proposed approach allows to divide the control problem into the internal states' control taking care of the DC-link balancing and the external states' control taking care of the load current regulation.

3.1 Modulation of the Multi-Active Bridge

The internal states control is achieved by the multi-active bridge. The goal is to keep the DC-link balanced, i.e. $V_{DC,1} = V_{DC,2}$. To achieve the DC-link balancing, the switches Q_i in Fig. 3 are used. Due to its strong self-balancing, in this paper, no external controller is added to the multi-active bridge and the system is balancing itself using only a modulator. Both active bridges, therefore, work in perfect synchronization. To produce a square-wave AC voltage at the midpoint and therefore keep the magnetic field of the multi-active bridge, the switches Q_{1i} and Q_{4i} must be closed at the same time and complementary to Q_{2i} and Q_{3i} as shown in Fig. 5. In this paper, no phase shift between the switches is applied and the duty cycle for all MOSFETs is equal to 0.5 at all times. Furthermore, the switching frequency must be high enough to prevent the transformer from going into saturation. To reduce switching losses, a zero voltage switching technique such as the one presented in [18] can be used.

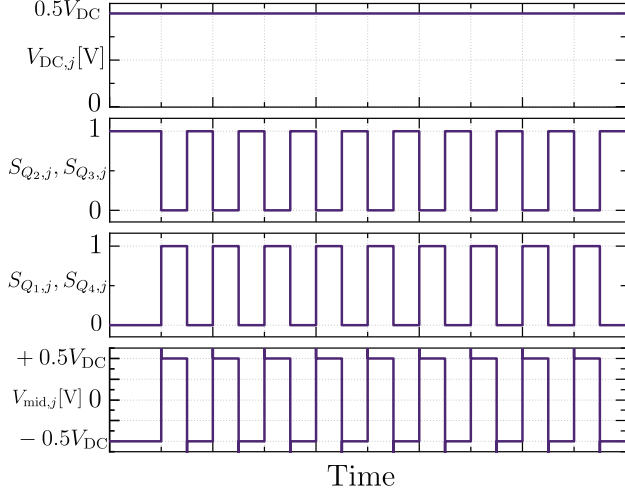


Fig. 5 Modulation of the switching signals for the multi-active bridge used in this paper. Shown are the transients of different voltages and switching in Fig. 3. S_k refers to the switching signal that is applied to the switch named k . The index j where $j \in \{1, 2\}$ for the examined system indicates which of the active bridges is shown.

3.2 Modulation and Control of the Neutral Point Clamped Inverter

The control of the load current is the task of the NPC phase leg. Therefore the switches G_{a1} to G_{a4} are used. A model predictive controller (see e.g. [19]) will be used to ensure that the output current follows a given reference. The input of the controller is the measured load current i_{load} and its given reference $i_{\text{load}}^{\text{ref}}$ and the output is the switching state S_a^{opt} of the NPC phase leg that would achieve the best reference tracking the performance of the load current. An overview of the relationship between the switching states and the output voltage is given in Table 1. Using the information from Table 1 and assuming

Table 1 Overview of the switching states of the NPC phase leg.

State S_a	S_{a1}	S_{a2}	S_{a3}	S_{a4}	V_{out}
1	1	1	0	0	$0.5V_{\text{DC}}$
0	0	1	1	0	0
-1	0	0	1	1	$-0.5V_{\text{DC}}$

the multi-active bridge provides perfect DC-link balancing we can express the output voltage V_{out} as

$$V_{\text{out}} = \frac{1}{2} S_a V_{\text{DC}}. \quad (1)$$

The derivative of the load current i_{load} is given by the load inductor differential equation as

$$\frac{d}{dt} i_{\text{load}} = \frac{V_L}{L_L}. \quad (2)$$

With the help of Kirchhoff's voltage law, we can express V_L in terms of V_{out} and the output resistor voltage V_R :

$$\frac{d}{dt} i_{\text{load}} = \frac{V_{\text{out}}}{L_L} - \frac{V_R}{L_L}. \quad (3)$$

Using Ohm's law on the output resistance as well as the switching-state voltage relationship this equation can be rewritten as

$$\frac{d}{dt} i_{\text{load}} = \frac{1}{2L_L} S_a V_{\text{DC}} - \frac{R_L}{L_L} i_{\text{load}}, \quad (4)$$

which describes the system dynamics. The above derivative expression can be approximated by a finite difference, using the Euler approximation:

$$\frac{d}{dt} i_{\text{load}} \approx \frac{i_{\text{load}}(t + T_s) - i_{\text{load}}(t)}{T_s}, \quad (5)$$

where T_s is the clock frequency of the controller. Applying the Euler approximation to the system dynamics yields the following expression:

$$i_{\text{load}}(t + T_s) = i_{\text{load}}(t) + T_s \cdot \left(\frac{V_{\text{DC}}}{2L_L} S_a - \frac{R_L}{L_L} i_{\text{load}}(t) \right). \quad (6)$$

With the help of a cost function $g(S_a)$ the deviation of the predicted current from its reference depending on the applied switching state is computed:

$$g(S_a) = \|i_{\text{load}}(t + T_s) - i_{\text{load}}^{\text{ref}}\|_2^2. \quad (7)$$

The goal is to obtain a switching state S_a^{opt} that the NPC phase leg can be in and that is furthermore minimizing the cost function $g(S_a)$. This is achieved by minimizing the following optimization problem:

$$S_a^{\text{opt}} = \arg \min g(S_a) \quad \text{s.t.} \quad S_a \in \{-1, 0, 1\}. \quad (8)$$

Due to the low number of candidate solutions, the optimization problem is solved using an exhaustive search. The procedure is repeated in the next clock cycle of the controller. Since the control of the external state is not required to uphold a magnetic field, a lower switching frequency can be used for the control of the external state.

4 Experiment Results

The proposed method was examined in an experimental setup. A DC-voltage of $V_{\text{DC}} = 200\text{V}$ was used to supply the NPC converter. The NPC has a DC-link capacitance of $C_{\text{DC}} = 517\mu\text{F}$. In addition to that, the controller clock frequency of the NPC was selected as $T_s = 5\mu\text{s}$. For the experimental setup, a multi-active bridge prototype presented in [18] was used. An overview over the prototype is shown in Fig. 6. To allow interleaving of the magnetics and compact power packaging, a planar structure with 16 windings was used. Each winding of the transformer has 6 turns. Since the proposed NPC phase leg only consists of two modules, the prototype is divided into two groups of 8

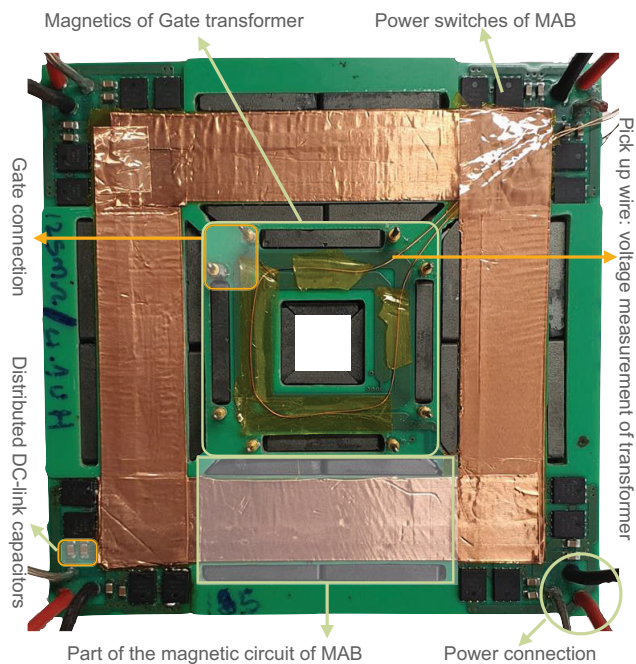


Fig. 6 Overview over the prototype used for the balancing part [18].

modules which will be connected in parallel to increase the current capacity. The multi-active bridge is connected to a gate driver which is tuned according to the guidelines presented in [18] and uses a switching frequency of 125 kHz which has been chosen experimentally as the one which yields the highest overall efficiency for the system. The series RL -load has a resistance of $R_L = 3.26\Omega$, and an inductance of $L_L = 4.997$ mH. The controller was programmed to follow a sinusoidal load current with an amplitude of 1.6 A and a frequency of 24 Hz was chosen. To assess the proposed method it is compared to the performance of the same DC-source, NPC and RL -load with no DC-link balancing. An overview of the experimental setup is shown in Fig. 7.

Figure 8 shows the result of the DC-link voltage balancing for the case of multi-active bridge based balancing and no DC-link balancing. It can be seen that while the multi-active bridge keeps the DC-link unbalance within 3% of V_{DC} , the same setup without balancing has a DC-link unbalance worse than 35% of V_{DC} .

A comparison of the load current is shown in Fig. 9. It can be seen that despite the high controller frequency and the controller putting all effort on the output load voltage the THD without balancing is still worse compared to the THD with balancing due to distorted output voltages.

5 Conclusion

This paper presented a novel balancing method for the DC-link voltages of a Three-level NPC converter. The aim was to balance the DC-link without having any influence on the performance of the output currents. This allows keeping the DC-link balanced while accessing the whole potential of the

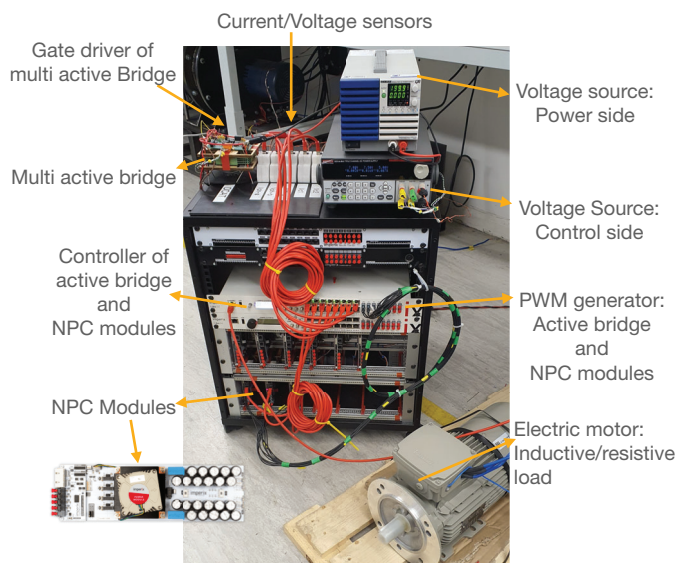


Fig. 7 Experimental setup used for the verification of the proposed topology. The setup is identical to the scheme shown in Fig. 4: An Imperix B-box shown in the center of the trolley was used as external controller and modulator. For the modulation of the multi-active bridge, a Spartan 6 FPGA (not shown) was used. The DC-source being connected to the multi-active bridge is seen on the top right, below of which is the auxiliary power source for the gate driver. A commercial NPC module where the auxiliary source was connected from the grid on the back side of the trolley was used for the setup. The NPC phase leg is shown on the lower part of the trolley and connected via optical wires to its controller. The multi-active bridge together with the gate driver is shown on the top left of the trolley. On the bottom right, a motor which was used as the RL -load can be seen. To evaluate the method, both AC-currents as well as DC-link voltages were recorded. The sensors for the recording are on the top center of the trolley.

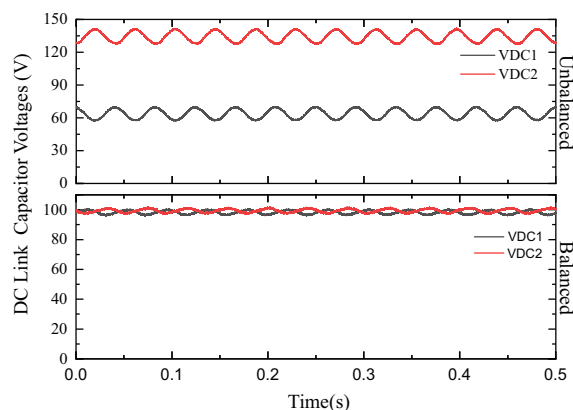


Fig. 8 DC-link balancing comparison between an unbalanced NPC and an NPC balanced with a multi-active bridge. The results for the multi-active bridge are shown in the lower subfigure while the result without balancing is shown in the upper subfigure.

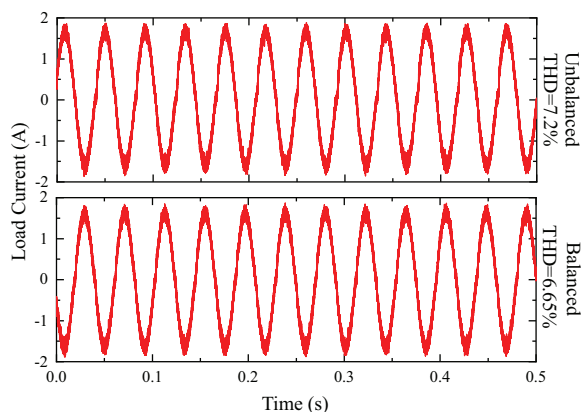


Fig. 9 Total harmonic distortion and AC-current comparison between an unbalanced NPC and an NPC balanced with a multi-active bridge.

topology. The control of the system can be distributed to internal and external state control. Using the structure of the system it is possible to solve both control problems independently from each other. To control the proposed system, a controller and two modulators were presented. Experiment results show the efficiency of the proposed system and the simplicity of the control.

References

- [1] A. Nabae, I. Takahashi, and H. Akagi, "A new neutral-point-clamped pwm inverter," *IEEE Transactions on Industry Applications*, vol. IA-17, no. 5, pp. 518–523, Sep. 1981.
- [2] Y. Ye and et. al., "Neutral-point-clamped five-level inverter with self-balanced switched capacitor," *IEEE Transactions on Industrial Electronics*, vol. 69, no. 3, pp. 2202–2215, 2022.
- [3] Y. Zhang and et. al., "An improved direct torque control for three-level inverter-fed induction motor sensorless drive," *IEEE Transactions on Power Electronics*, vol. 27, no. 3, pp. 1502–1513, 2012.
- [4] J. Reimers and et. al., "Automotive traction inverters: Current status and future trends," *IEEE Transactions on Vehicular Technology*, vol. 68, no. 4, pp. 3337–3350, 2019.
- [5] H. du Toit Mouton, "Natural balancing of three-level neutral-point-clamped pwm inverters," *IEEE Transactions on Industrial Electronics*, vol. 49, no. 5, pp. 1017–1025, Oct 2002.
- [6] R. Tallam, R. Naik, and T. Nondahl, "A carrier-based pwm scheme for neutral-point voltage balancing in three-level inverters," *IEEE Transactions on Industry Applications*, vol. 41, no. 6, pp. 1734–1743, 2005.
- [7] P. Kolahian and et. al., "Multi-port dc–dc converter for bipolar medium voltage dc micro-grid applications," *IET Power Electronics*, vol. 12, no. 7, pp. 1841–1849, 2019.
- [8] V. Jayakumar, B. Chokkalingam, and J. L. Munda, "A comprehensive review on space vector modulation techniques for neutral point clamped multi-level inverters," *IEEE Access*, vol. 9, pp. 112 104–112 144, 2021.
- [9] F. Donoso and et. al., "Finite-set model-predictive control strategies for a 3l-npc inverter operating with fixed switching frequency," *IEEE Transactions on Industrial Electronics*, vol. 65, no. 5, pp. 3954–3965, 2018.
- [10] M. Saedifard, R. Iravani, and J. Pou, "Analysis and control of dc-capacitor-voltage-drift phenomenon of a passive front-end five-level converter," *IEEE Transactions on Industrial Electronics*, vol. 54, no. 6, pp. 3255–3266, 2007.
- [11] R. Stala, "Application of balancing circuit for dc-link voltages balance in a single-phase diode-clamped inverter with two three-level legs," *IEEE Transactions on Industrial Electronics*, vol. 58, no. 9, pp. 4185–4195, 2011.
- [12] A. A. Boora, A. Nami, F. Zare, A. Ghosh, and F. Blaabjerg, "Voltage-sharing converter to supply single-phase asymmetrical four-level diode-clamped inverter with high power factor loads," *IEEE Transactions on Power Electronics*, vol. 25, no. 10, pp. 2507–2520, 2010.
- [13] J. Hachlowski and R. Stala, "Dc-link voltage balancing converter with resonant switched-capacitor circuit for four-level and six-level npc inverter," in *2019 21st European Conference on Power Electronics and Applications (EPE '19 ECCE Europe)*, 2019, pp. P.1–P.10.
- [14] Y.-M. Chen, Y.-C. Liu, and F.-Y. Wu, "Multi-input dc/dc converter based on the multiwinding transformer for renewable energy applications," *IEEE Transactions on Industry Applications*, vol. 38, no. 4, pp. 1096–1104, 2002.
- [15] F. Grimm, M. Baghdadi, and R. Bucknall, "An n-port system model for multiwinding transformer based multilevel converters in dc-autotransformer configuration," in *2021 IEEE Design Methodologies Conference (DMC)*, 2021, pp. 1–6.
- [16] J. Wood and et. al., "Adiabatic dc-ac power converter with 99% efficiency," in *PCIM Europe 2016: Proceedings of International Exhibition and Conference for Power Electronics, Intelligent Motion, Renewable Energy and Energy Management*. IEEE, 2016, pp. 1–8.
- [17] D.-J. Park and et. al., "A novel battery cell balancing circuit using an auxiliary circuit for fast equalization," in *IECON 2014 - 40th Annual Conference of the IEEE Industrial Electronics Society*, 2014, pp. 2933–2938.
- [18] F. Grimm, P. Kolahian, J. Wood, R. Bucknall and M. Baghdadi, "An isolated gate driver for multi-active bridges with soft switching," Arxiv Preprint, <https://arxiv.org/abs/2204.01547>, 2022.
- [19] A. G. Bartsch and et. al., "A comparison among different finite control set approaches and convex control set model-based predictive control applied in a three-phase inverter with rl load," in *2019 IEEE 15th Brazilian Power Electronics Conference and 5th IEEE Southern Power Electronics Conference (COBEP/SPEC)*, 2019, pp. 1–6.